Journal of Materials Chemistry B

Accepted Manuscript

ROYAL SOCIETY OF CHEMISTRY

www.rsc.org/materialsB

Development of zwitterionic copolymers with multi-shape memory effects and moisture-sensitive shape memory effects

Shaojun Chen[1*], Funian Mo[1], Florian J Stadler[1],Shiguo Chen[1], Zaochuan Ge[1], Haitao Zhuo[2*],

[1]*Shenzhen Key Laboratory of Special Functional Materials, Nanshan District Key Lab for Biopolymers and Safety Evaluation, College of Materials Science and Engineering, Shenzhen University, Shenzhen, 518060, China.* [2]*College of Chemistry and Chemical Engineering, Shenzhen University, Shenzhen, 518060, China.*

*Corresponding author: College of Materials Science and Engineering，Shenzhen University, Shenzhen 518060, China. Tel and Fax: +86-755-26534562. E-mail: S.J.Chen, chensj@szu.edu.cn; H.T.Zhuo, haitaozhuo@163.com;

Abstract

Shape memory polymer (SMP) and zwitterionic polymer both have great applications in biomedical fields. This paper successfully combines functionalities of zwitterionic polymer and SMP, developing new kind of zwitterionic copolymer having multi-shape memory effect (SME) and moisture-sensitive SME. The results demonstrate that a series of zwitterionic multi-SMPs, coded as p(DMAPS-co-AA), were synthesized from DMAPS and acrylic acid (AA). Micro-phase separated structure is formed in the resulting p(DMAPS-co-AA). The strong hydrogen bonding between AA segments serves as reversible switch, while the strong electrostatic forces among DMAPS segments serve as physical crosslinkers. Therefore, shape memory testing demonstrates that the p(DMAPS-co-AA) shows not only dual-SME, but also triple-SME and quadruple-sSME. Moreover, in addition to the thermal-induced SME, p(DMAPS-co-AA) also shows moisture-sensitive SME. It is thus proposed that this zwitterionic multi-SMP could find great potential applications in smart biomedical fields.

Keywords: Zwitterionic Polymer; Shape memory polymer; Multi-shape memory effect; Moisture-sensitive shape memory effect; Biomedical application;

1. Introduction

Shape memory polymers (SMPs) are those polymeric smart materials with the capability of fixing a temporary shape and recovering to its original shape in response to the application of a specific stimulus like heat, light, pH and water.[1-6] Recently, SMPs have become increasingly important due to the growing number of applications, such as actuators,[7, 8] biomedical devices,[9] smart clothing,[10] flexible electronics, aircraft devices.[11, 12] information carriers,[13] assembly/disassembly.[14, 15] Thermal-responsive SMPs can be used in most of their applications since their shape recovery is generally triggered by heating the specimen above a transition temperature. However, the pre-stored strains are expected to be recovered without external heating in the biomedical applications.[16] Thus, SMPs triggered by water or moisture would be more suitable for biomedical applications.[17, 18] Huang and co-workers had studied systematically water-driven shape memory polyurethane.[18] Jung *et al*. also observed water-responsive SMEs in poly(ethylene glycol) (PEG)-based polyurethane modified with polyhedral oligomeric silsesquioxane. Zhu *et al.* had prepared one kind of rapidly switchable water-sensitive shape memory cellulose/elstomer nanocomposites.[19] Wang *et al.* recently had also reported the water-induced SMEs and its mechanism in the sodium dedecylsulfate/epoxy composite.[20] Chen *et al.* had also synthesized one kind of supramolecular polyurethane showing moisture-sensitive SMEs.[17] These recent findings of moisture-sensitive SMPs greatly promote the development and applications of SMPs. This concept was also proposed to deliver biomedical device into living cells in future.[16] However, the biocompatibility of SMPs should be further improved before the SMPs are used as various biomaterials. In this study, we propose another kind of moisture-sensitive SMPs by using zwitterioinc polymer with good biocompatibility.

On the other side, recent research of SMPs also tends to develop multi-shape memory effect (SME), which can fix two or more temporary shapes and recover from the first temporary shape to the other temporary shapes one by one, until ultimately finally obtaining a permanent shape.[21-23] SMPs with multi-SME, called as multi-SMPs, are believed to have significant and broad technology impacts. The key factor to realize multi-SMEs is the integration of two or more reversible phases into a polymer network. [21-23] One strategy is to incorporate several discrete thermal transitions into the material.[1] For instances, triple-memory properties could be achieved by designing two thermal transitions in

multi-block segmented polyurethanes,[24-26] grafting polymers,[27, 28] semi-interpenetrating polymer networks,[29] polymer blends,[30, 31] or polymer composites.[32] Another strategy relies on a single broad thermal transition since the broad thermal transition could be thought to multiple distinct transitions.[33] Xie and Li had achieved step-wise multi-shape memory and recovery by using the broad α-transition in perfluroosulphonic acid ionomers (PFSA).[23, 34] Though many kinds of multi-SMPs have been reported previously, PFSA is still a very important thermoplastic multi-SMPs which can be processed into thin films for building bulk smart devices.[35] Another important multi-SMP is a polyethylene-based carboxylate (PEMA) ionomer, which is a semi-crystalline ionomer with a broad melting temperature range.[36] The similarities in structure for PFSA and PEMA exhibiting multi-SMEs consists of long ionic side chains, providing a broad transition and forming a "semi-permanent" cross-linked network using ionic clusters. However, up to date, the reported ionic polymers having SME are limited to polyelectrolytes, which contain only anionic or cationic groups. In this study, we would like to develop another new kind of multi-SMPs from zwitterionic polymers containing both anionic and cationic groups.

Zwitterionic polymers have attracted significant interest as biomedical materials.[37-39] Particularly, zwitterionic sulfobetaine polymers show high resistance to non-specific protein adsorption due to high hydration capacity and neutral charge surface.[40] Surface modification with zwitterionic sulfobetaine polymers greatly reduces fibrinogen adsorption, platelet adhesion, bacterial adhesion, and plasma coagulation.[41] Some zwitterionic sulfobetaine polymers even show good antimicrobial properties due to a large number of quaternary ammonium groups [42] or sulfonate groups allowing for further incorporation of antimicrobial silver ions.[43] In recent years, zwitterionic polymers have also been designed for stimuli-responsive polymer systems due to their reversible responsiveness to changes in temperature, chemical reactions, ionic strength, specific ion pairing, and/or, more rarely, changes in pH.[44] Particularly, recently developed electrolyte-responsive zwitterionic membranes and pH-sensitive zwitterionic micelles show many promising applications in protein purification and drug delivery.[45, 46] However, little has been reported on zwitterionic SMPs, which are expected to have good biocompatibility since zwitterionic polymers are noncytotoxic, biocompatible, and biomimetic,[47-49] leading to several promising biomedical

applications, such as in drug delivery,[40] wound dressing,[43, 50] nonadherent coatings,[51] and protein separation.[52]

In an earlier communication, we had successfully developed one kind of zwitterionic polyurethane for shape memory materials by two-step reactions.[53] In addition to the multi-SME, the zwitterionic polyurethane also shows good self-healing properties. In the present study, we would like propose another strategy to prepare new kind of multi-SMPs by free radical polymerization method using zwitterionic monomer, 3-dimethyl (methacryloyloxyethyl) ammonium propane sulfonate (DMAPS).[54-57] In this experiment, a series of zwitterionic copolymers, called as p(DMAPS-co-AA), were synthesized from DMAPS and acrylic acid (AA). Thereafter, the structure, morphology and properties, particularly the thermal-induced multi-SME and moisture-sensitive SMEs are investigated systematically.

2. Experimental Section

2.1 Materials:

3-Dimethyl (methacryloyloxyethyl) ammonium propane sulfonate (DMAPS, CAS.#537284) was synthesized by Changzhou Yipingtang Co. Ltd. (Changzhou, China). Acrylic acid (AA, CAS.#174230), ammonium persulphate ($(NH_4)S_2O_8$, CAS.#7727540) and other chemicals were purchased from Aladdin (Shanghai, China).

2.2 Synthesis of p(DMAPS-co-AA)

p(DMAPS-co-AA) was synthesized with DMAPS and AA by radical polymerization method according to the composition on Table 1. Typically, the preparation was performed in a nitrogen filled and mechanically stirred 500 ml three-neck flask. After the monomers (e.g. 20.0g DMAPS and 80.0g AA) were added to the flask, the polymerization was initiated by addition of 5 mM ammonium persulphate into the monomer solution, which proceeded at 70°C for 10h under constant stirring **(see Figure 1)**. Finally, samples were prepared after water was evaporated from the resulting 20 wt.% polymer solution in a Teflon pan at 80°C for 24h in continuous air flow and then *in vacuum* for another 24h. In this study, the sample names were coded as DMAPS#, in which "#" refers to the weight percentage of DMAPS-content in feed ratio, e.g. DMAPS20.

Table 1. Composition of synthesized DMAPS-co-AA copolymer

Sample	feed ratio (AA:DMAPS)	Elemental Composition (At.%)				DMAPS-content (wt.%) calculated by	
		N	C	S	O	EA*	^{1}H-NMR**
DMAPS20	8:2	4.54	47.60	2.22	37.00	19.41	21.73
DMAPS30	7:3	4.75	46.70	3.31	35.00	28.95	28.61
DMAPS40	6:4	4.92	47.49	3.85	34.94	33.70	35.32
DMAPS50	5:5	4.74	46.51	5.15	35.80	45.00	41.72
DMAPS60	4:6	4.58	47.55	6.67	37.50	58.28	51.20

*EA: Elemental Analyzer; **^{1}H-NMR: ^{1}H-Nuclear Magnetic Resonance

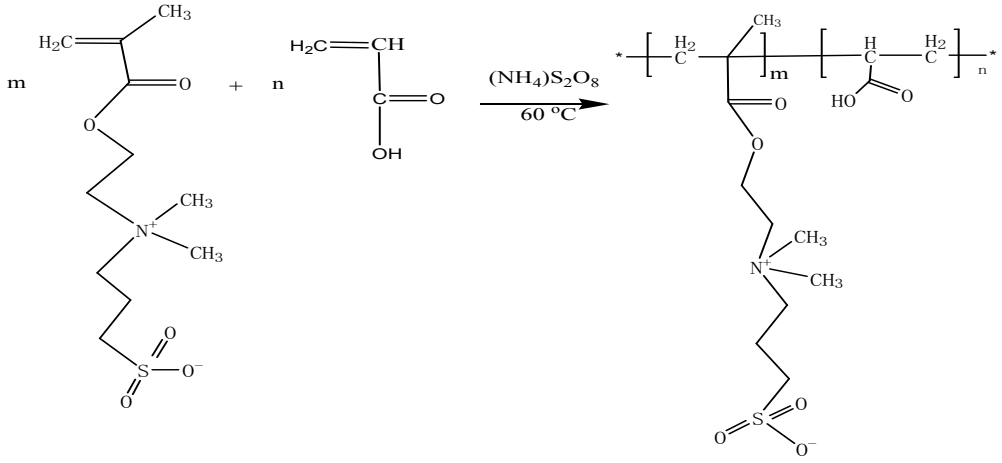

Figure 1. Polymerization reaction of DMAPS-co-AA copolymers

2.3 Materials Characterizations

ATR-FTIR spectra were recorded with a Nicolet 760 FT-IR spectrometer equipped with an ATR accessory MUP with GeS crystal. 24 scans at 4 cm^{-1} resolution were signal averaged and stored as data files for further analysis.

The ^{1}H-NMR spectrum was recorded with Avance-400Hz (Bruker) with D_7-DMF as the solvent and tetramethylsilane (TMS) as internal standard.

The weight percentages of C, H, N and S of the samples were determined using a Vario EL Ø elemental analyzer (EA, Germany, Elementar).

The XPS analysis was made on a VG multilab2000 with Al Kα source. The anode voltage was 15KV and the anode current was 10mA. The core-level signals were obtained at

a photoelectron take-off angle of 90º. The elemental compositions were determined on the basis of peak areas and sensitivity factor from the C_{1s}, N_{1s}, O_{1s} and S_{2p} peaks by advantage software. All binding energy values were determined with reference to carbon, C1s=284.6eV.

DSC testing was carried out by using a TA Q200 instrument having nitrogen as the purged gas. Indium and zinc standards were used for calibration. Samples were firstly heated up from -60 °C to 150°C at a heating rate of 10°C/min and kept at 150 °C for 1 min, subsequently, cooled to -60°C at a cooling rate of 10°C/min, and finally the second heating scan from -60°C to 150°C was performed again.

TGA curves were recorded after drying at 100°C on a computer-controlled TA Instrument TG Q50 system, under the following operational conditions: heating rate 10 °C/min, temperature range 100-600°C, sample weight about 5.0mg, using a film sample in platinum crucibles under N_2 flow (60 ml/min). In order to get a good accuracy, exact experiment was repeated at least 3 times and averaged.

Modulus testing was carried out by a computer-controlled TA Instrument DMA800 system. Specimens were cut from sample film with thickness of 0.5 mm, and the distance between two clamps is 10 mm in the initial testing status. Specimens were determined under 1.0 Hz and a heating rate of 2.0 K/min.

Nanonavi E-Sweep (SII Nanotechnology Inc.) atomic force microscopy (AFM) was used in tapping mode for morphological characterization of the dried sample. The samples were dissolved in DMF at a concentration of 5 mg/ml and spin-coated firstly at 400 rpm for 10 s and then 4000rpm for 60 s on oxidized silicon substrates. Spin-coated films were kept in a 50 °C oven for 48 h to evaporate the solvent.

The moisture absorption was determined by weighing the specimens on a balance, as described in ref. [58]. Before testing, the specimens with a thickness of 1.0 mm were dried completely. The specimen was then put on the moisture condition with a certain RH and a certain temperature. The moisture absorption in percentage as a function of time (M_t(t)) is calculated from the weight increase.

2.4 Multi-Shape-Memory Behavior Testing

The thermal-induced multi-shape-memory behaviors were determined with thermo-mechanical analysis using a TA Instruments DMA800 (using tension clamps in controlled

force mode) according the procedure described in ref..[53] All samples were dried at 100°C *in vacuo* for 24h and cut in rectangular pieces of approximately 10mm×2.0mm×0.5mm. The detail test setup for dual-shape-memory cycles, triple-shape-memory cycles and quadruple-shape-memory cycles are provided below.[36]

a) For dual-shape-memory cycles: (1) heating to ca. 90°C followed by equilibration for 20 min; (2) uniaxial stretching to strain (ε_{load}) by ramping force from 0.001N to 1N at a rate of 0.25N/min; equilibration for 3 min; (3) fixing the strain (ε) by rapid cooling to ca. 20°C with q=-10°C/min, followed by equilibration for 10min; (4) unloading external force 0N at a rate of 0.25N/min; (5) reheating to ca.90°C at a rate of 4°C/min and followed by equilibration for 40min; the recovery strain (ε_{rec}) is finally recorded.

b) For triple-shape-memory cycles: (1) heating to ca. 100°C and equilibrated for 20 min; (2) uniaxial stretching by ramping force from 0.001N to 1N at a rate of 0.25N/min; equilibration for 3 min; (3) fixing the strain by rapid cooling to 70°C with q=-10°C/min, followed by equilibration for 10min; (4) further fixing the strain by rapid cooling to 20°C with q=-10°C/min, followed by equilibration for 10min; (5) unloading external force 0N at a rate of 0.25N/min; (6) reheating to 70°C at a rate of 4°C/min and followed by equilibration for 40min; (7) reheating to ca. 100°C at a rate of 4°C/min and followed by equilibration for 40min.

c) For quadruple-shape-memory cycles: (1) heating to 110°C and equilibrated for 20 min; (2) uniaxial stretching by ramping force from 0.001N to 1N at a rate of 0.25N/min; equilibration for 3 min; (3) fixing the strain by rapid cooling to 90°C with q=-10°C/min, followed by equilibration for 10min; (4) further fixing the strain by rapid cooling to 70°C with q=-10°C/min, followed by equilibration for 10min; (5) further fixing the strain by rapid cooling to 0°C with q=-10°C/min, followed by equilibration for 10min; (6) unloading external force 0N at a rate of 0.25N/min; (7) reheating to 70°C at a rate of 4°C/min and followed by equilibration for 40min. (8) further reheating to 90°C at a rate of 4°C/min and followed by equilibration for 40min. (9) further reheating to 110°C at a rate of 4°C/min and followed by equilibration for 40min.

d) For sequential shape recovery: (1) heating to 120°C and equilibrated for 20 min; (2) uniaxial stretching by ramping force from 0.001N to 1N at a rate of 0.25N/min; equilibration

for 3 min; (3) fixing the strain by rapid cooling to 0°C with q=-10°C/min, followed by equilibration for 10min; (4) unloading external force 0N at a rate of 0.25N/min; (5) reheating to 60°C at a rate of 4°C/min and followed by equilibration for 40min. (6) further reheating to 80°C at a rate of 4°C/min and followed by equilibration for 40min. (7) further reheating to 95°C at a rate of 4°C/min and followed by equilibration for 40min. (8) further reheating to 110°C at a rate of 4°C/min and followed by equilibration for 40min.(9) further reheating to 120°C at a rate of 4°C/min and followed by equilibration for 40min.

2.5 Moisture-Sensitive Shape Memory Behavior Testing

Strain recovery *versus* immersion time curve is used to characterize the moisture-sensitive shape recovery behavior.[59] The detail test setups are provided below. Before testing, the specimens with a thickness of 1.0mm, a width of 5.0mm, a length of 20.0mm (L_0=20mm) were dried at 100°C *in vacuo* for 24 hours, The specimens were stretched to a certain maximum elongation (L_{max}) at finite temperature beyond T_{trans}, e.g. 60°C. After they were fixed at a low temperature (e.g. 20°C) to a deformed strain (L_f), the deformed specimen was conditioned at a constant RH (e.g. 80% RH). The length at any time (L_t) was then recorded each 10 minutes under the constant moisture condition. Finally, similar to the calculation method of thermal-induced SMEs described in literature,[60] the moisture-sensitive strain recovery at any time (R_t) was calculated using equation (1).

$$R_t = (L_f - L_t)/(L_{max} - L_0) \times 100\% \quad \text{.....(1)}$$

Hence, the curve of strain recovery (R_t) *versus* immersion time (t) was obtained and used for characterizing the moisture-sensitive SMEs. Three specimens were tested in parallel. When the three curves are very close to each other, the obtained curves were taken for further analysis in each sample.[59]

3. Results and Discussions

3.1 Structure Analysis

The molecular structure of p(DMAPS-co-AA) was firstly investigated with ATR-FTIR (**Figure 2A**) and XPS **(Figure 2B**). The sulfobetaine structure is confirmed by the presence of SO_3^- at 1035 cm^{-1} in both pure DMAPS and the copolymer. The broad peaks centred at ≈1709 cm^{-1} and ≈1639 cm^{-1} proves the successful copolymerization of DMAPS with AA (**Figure 2A**). The DMAPS content determined by elemental analysis and ^{1}H-NMR (**Figure**

SI1) also matches the feed very well, despite a degree of uncertainty due to residues from the initiator $NH_4S_2O_8$. Additionally, the XPS survey scan spectra demonstrate that S_{2p} (binding energy 166 eV) and N_{1s} (binding energy 400 eV), which are two indicative atoms for DMAPS, are detected in p(DMAPS-co-AA) (**Figure 2B**). Furthermore, the N_{1s} spectrum consists of two peaks, one peak at 402 eV for the sulfobetaine ammonium nitrogen ($-N^+(CH_3)_2CH_2$) and the other peak at 400 eV for the nitrogen in the NH_4^+ cations from $(NH_4)S_2O_8$ serving as the initiator because sulfobetaine ammonium nitrogen ($-N^+(CH_3)_2CH_2$) was only measured in the N_{1s}-spectrum of pure DMAPS **(Figure SI2)**. The C_{1s} superfine scan spectrum further shows three main peaks with binding energies at 284.8, 285.9, and 288.8 eV, corresponding to carbon atoms of saturated hydrocarbons (-C-C-); carbon atoms with a single bond to oxygen (-C-O-), nitrogen (-C-N-), or sulphur (-C-S-); and carbon atoms in carbonyl groups (-C=O-)[61] (**Figure 2B-** the inner spectra). It is, thus, confirmed that DMAPS are copolymerized with AA successfully to form DMAPS-co-AA copolymer containing sulfobetaine groups.

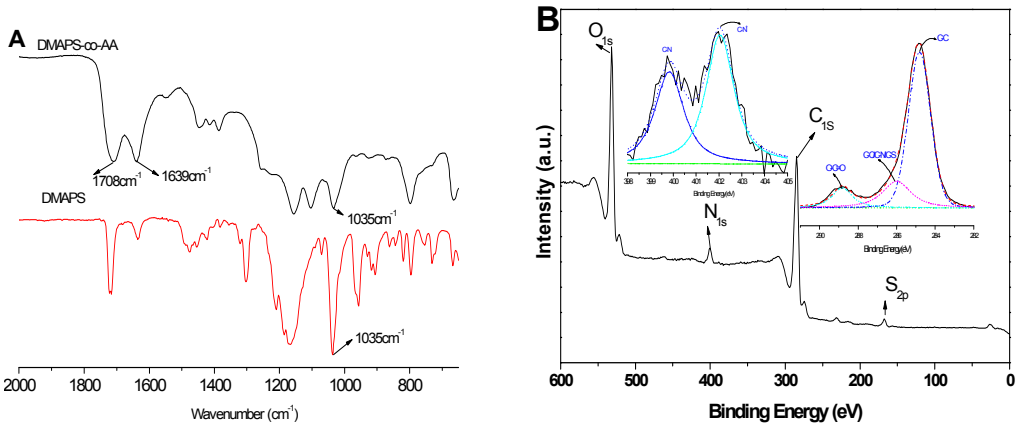

Figure 2. Molecular structure analysis of DMAPS-co-AA copolymer. (A) ATR-FTIR spectra; (B) XPS spectra

3.2 Thermal properties

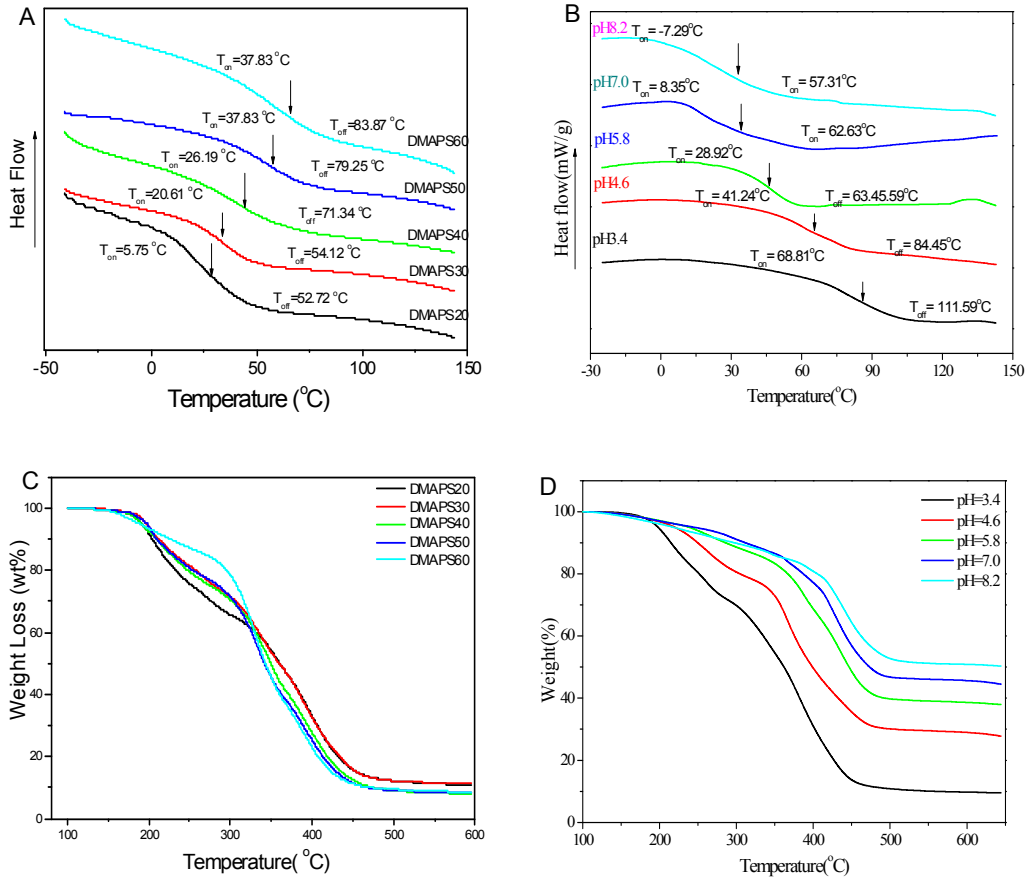

Figure 3. Thermal properties of DMAPS-co-AA copolymers (A - second DSC heating curves of copolymers with various DMAPS content; B - second DSC heating curves of sample DMAPS20 at different pH; C - TGA curves of the copolymers at varying DMAPS contents; D - TGA curves of DMAPS20 at different pH)

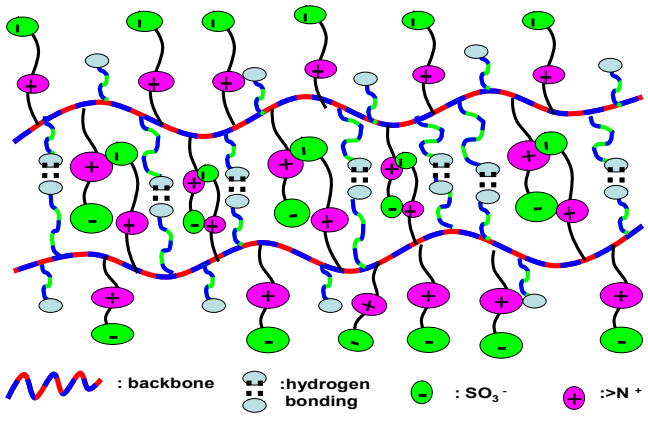

Figure 4. Illustration for molecular structure of DMAPS-co-AA copolymer

Thermal properties of DMAPS-co-AA copolymers were investigated with DSC and

TGA (**see Figure 3**). One obvious glass transition temperature (T_g) was detected by DSC in all samples, e.g., 29.5°C for DMAPS20 and 65.5°C for DMAPS60 (**Figure 3A**). Considering the onset and offset value, all samples show a broad glass transition with significant change in specific heat capacity (ΔC_p), presumably because of a broad mixing phase on the interface of hard phase and soft phase. The T_g as well as the onset and offset temperature all increase linearly with an increasing DMAPS content **(Figure SI3)**. The effect of DMAPS is similar to the hard segment of the common segmented polyurethanes with thermal-induced SME.[60] This result indicates that the DMAPS-rich domains consisting of strong electrostatic inter/intra-chain associations significantly influence the movement of the polymer chains, serving as hard domains or physical cross-links. By changing the pH value of sample DMAPS20 with addition of sodium hydroxide solution, the glass transition of polymer chain is also influenced greatly. **Figure 3B** demonstrates that as the pH increases from 3.4 to 8.2, the T_g of p(DMAPS-co-AA) shifts to lower temperature and the ΔC_p also increases, suggesting weakening of the hydrogen bonding among AA segments due to the pH increase,[62] leading to varied chain mobility or morphology. By contrast, the zwitterionic interactions are not significantly affected by pH.[44] Additionally, the TGA curves provide another proof to the molecular structure of DMAPS-co-AA copolymer. **Figure 3C** demonstrate that the onset decomposition temperature (T_i) of samples with lower DMAPS-content tends to be lower than that of sample with higher DMAPS-content; whereas the offset decomposition temperature (T_e) is higher for lower DMAPS-contents. Moreover, a higher pH increases the thermal stability of p(DMAPS-co-AA) and the amount of residue due to the higher sodium salt (F**igure 3D**). This result suggests that the DMAPS segments show better thermal stability than AA segments. The thermal stability of p(DMAPS-co-AA) is enhanced by DMAPS-segments. It also suggest that the electronic structure of p(DMAPS-co-AA) is changed greatly by pH because the thermal decomposition of vinyl polymers including AA-based copolymers is ascribed to depolymerisation,[63] which may be greatly influenced by sodium ions.[64] It is, thus, confirmed again that p(DMAPS-co-AA) is composed of two segments: AA segments and DMAPS segments. The strong hydrogen bonds among AA segments serve as reversible switches, while the strong electrostatic forces among DMAPS segments serve as physical netpoints (**see Figure 4**). This hypothesis was further confirmed

from the temperature-dependent FT-IR spectra (**see Figure SI4**). As the temperature increases, the OH deformation vibration frequency shifts from 1165cm^{-1} to 1153 cm^{-1} while the C=O stretching frequency shifts from 1723 to 1736cm^{-1}, suggesting weakening of the hydrogen bonding among AA segments due to the temperature increase.[65]

3.3 Mechanical and Morphology Analysis

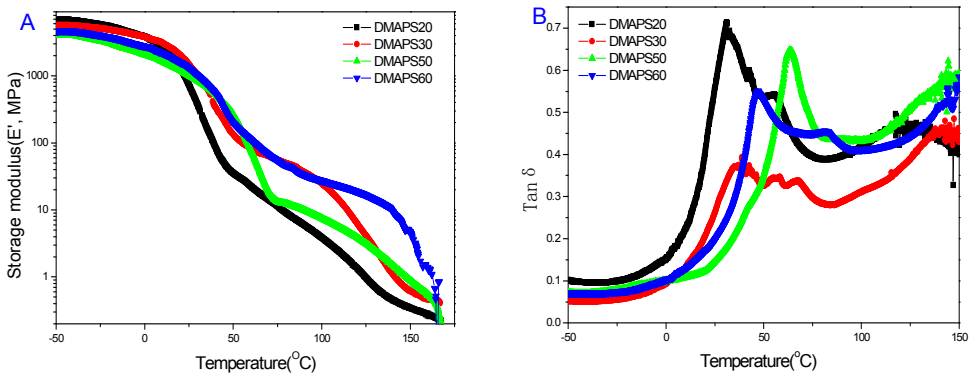

Figure 5. DMA curves (A – storage modulus E' curves and B – damping factor tanä dependence on temperature) of DMAPS-co-AA copolymers

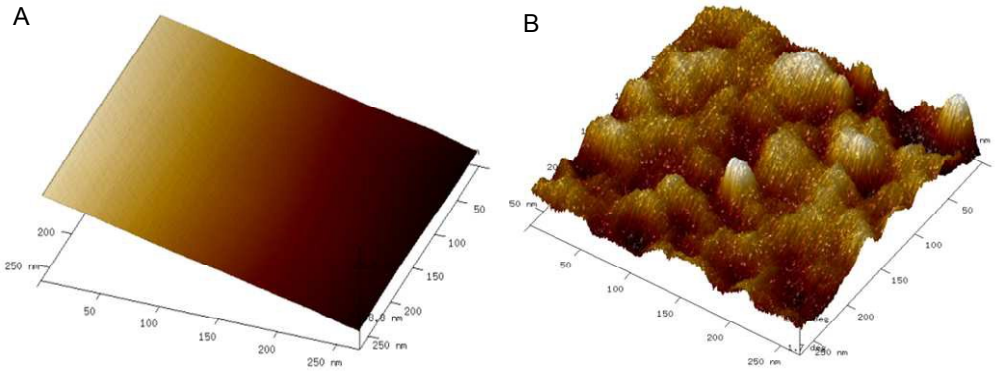

Figure 6.AFM images (A- 3D height, B-3D phase) of sample DMAPS20

DMA curves of p(DMAPS-co-AA) provide a powerful proof to its micro-phase morphology. The DMA data prove that the phase transition identified in DSC is the glass transition of polymer because the ratio between glassy and rubber modulus is up to 300 (**Figure 5A**). The trend from thermal data (Figure 3A), in which T_g increases with increasing DMAPS content, is also confirmed. As the temperature continuously increases, a second modulus change occurs above 100°C in all copolymers. The fact that the materials become too soft to be measured properly above >120°C also proves the high molar mass of the samples and the absence of sizable cross-linking, as a long rubbery plateau but finite is the

fingerprint of a high molecular uncrosslinked material.[66] The corresponding two T_g values can be determined from the maxima of the tanä curves, e.g., 30.7°C and 124.8°C for DMAPS20, implying the formation of a micro-phase separation structure (**Figure 5B**). Furthermore, a typical AFM image confirms the formation of dual-phase separated structure composed of a hard phase and a soft phase (**Figure 6A-B**). Together with the AFM 2D-image (**Figure SI5**), the DMT-Modulus 3D-images clearly show some cuspidal outshoots, which may be zwitterion-rich aggregates serving as hard phase, and some pot holes ascribed to the soft phase of p(DMAPS-co-AA),[18] which satisfies the precondition for good shape memory properties. Moreover, the wide double glass transition ranging from 25 to 100°C might provide multiple reversible transitions to the p(DMAPS-co-AA), allowing it to exhibit multi-shape-memory effects.[23, 67]

3.4 Thermal-induced SME

To qualitatively test the SME, an "E"-shaped specimen of DMAPS20 was prepared and then deformed to a temporary "I"-shape by heating to 80°C followed by fixing at ambient temperature. In a second heating process, the "E"-shape started recovering at ≈50°C, reaching the original shape at ≈80°C (**Figure 7A**), which was a typical thermal-induced shape-memory-recovery process.[3] These results were further quantified by cyclic tensile tests (**Figure SI6**), which is widely used to characterize the thermal-induced SME.[68] Further tests verified that all of the samples have very good shape fixity >90%, while the shape-recovery decreases as the DMAPS content increases (**Figure 7B**). Possibly, DMAPS as a hard segment in p(DMAPS-co-AA) along with the strong electrostatic inter/intra-chain associations are responsible for this behaviour, which is relatively similar to the effects of the hard segment in shape-memory polyurethanes. Hence, as the hard segment content increases, random synthesis becomes less likely, which may reduce the shape-recovery.[60] Thus, similar to shape-memory polyurethanes,[60] the thermal-induced shape-memory properties of p(DMAPS-co-AA) can also be adjusted by changing the DMAPS-content. Particularly, p(DMAPS-co-AA) with lower DMAPS-content, e.g. DMAPS20, have both good shape fixity and shape recovery (**Figure 7C**).

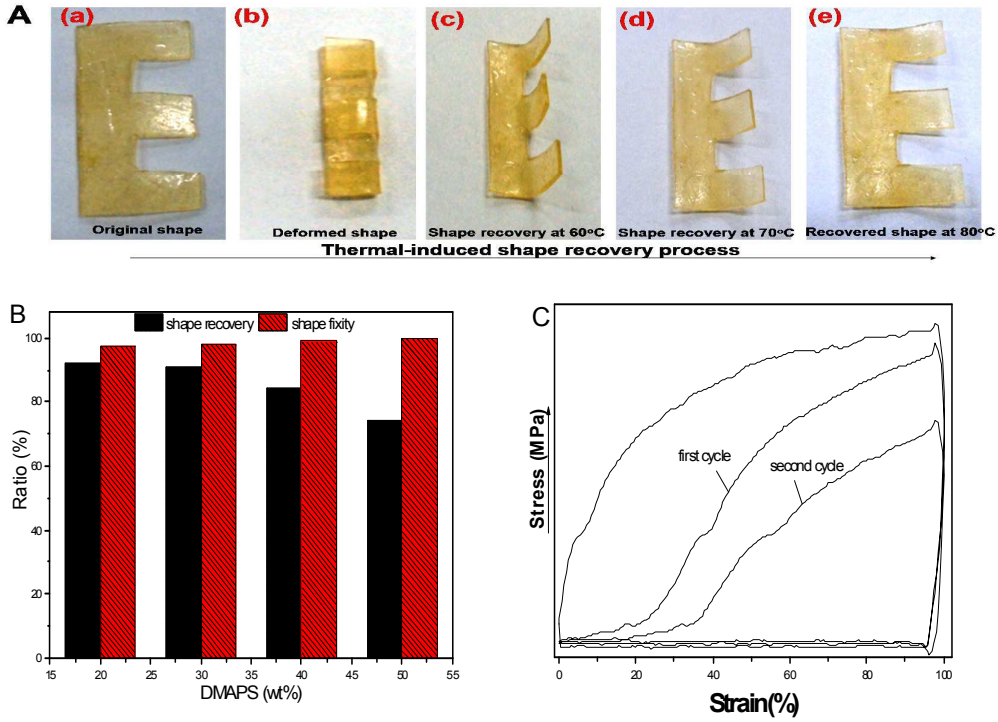

Figure 7. Thermal-induced dual-SME of DMAPS-co-AA copolymers (A - thermal-induced shape recovery process of sample DMAPS20; B - shape fixity and shape recovery of p(DMAPS-co-AA) with various DMAPS-content; C - strain-stress cyclic curves of sample DMAPS20)

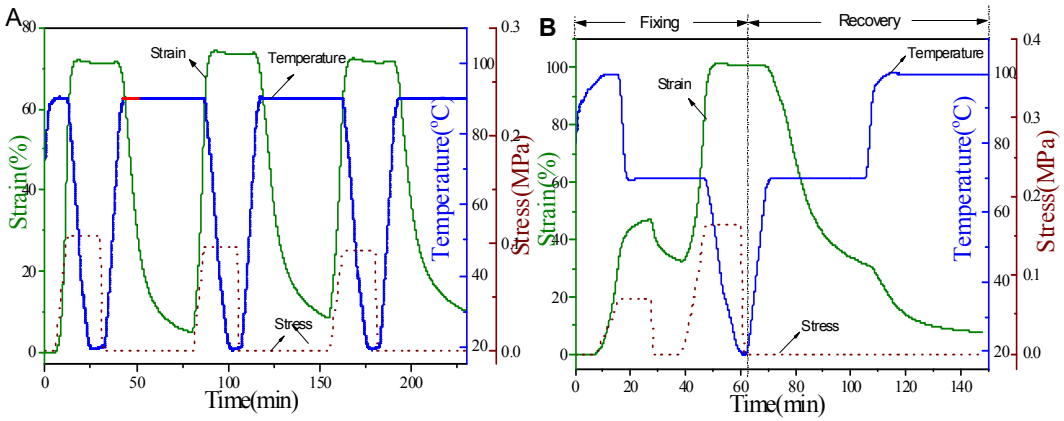

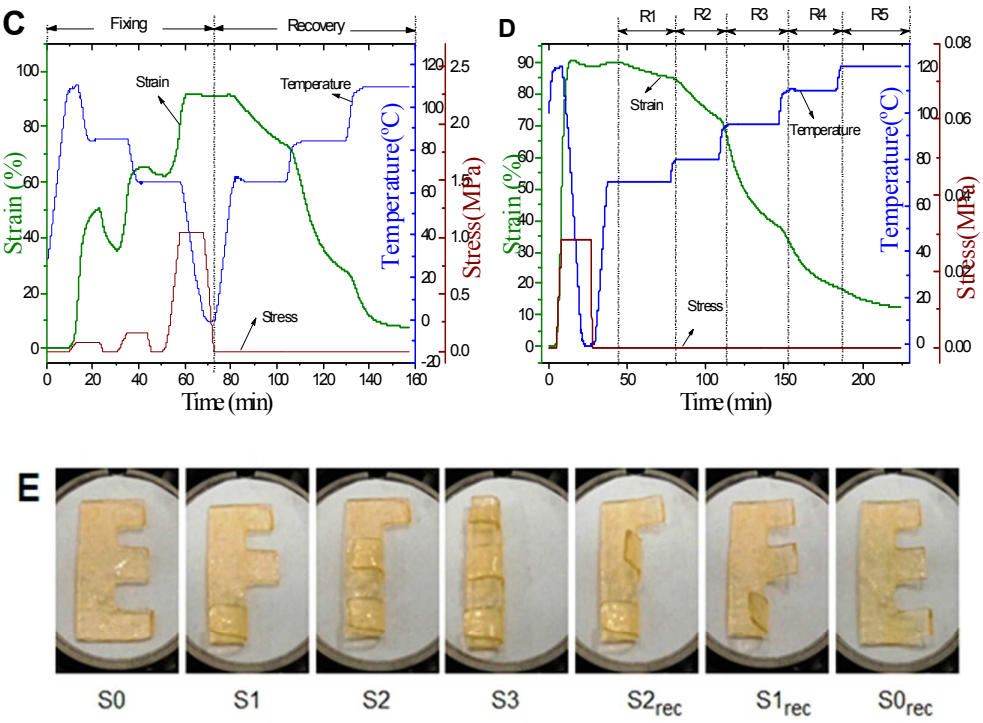

Figure 8. Thermal-induced multi-SMEs of DMAPS-co-AA copolymers A) repeated dual-SME; B) triple-SME; C) quadruple-SME; D) sequential shape recovery; E) a group of photos showing the sequential fixed at 110°C; 90°C and 70°C; recovered at 90°C and 110°C.

The thermal-induced shape memory properties could also be determined with thermo-mechanical analysis using tension clamps in controlled force mode. **Figure 8A** demonstrates that 96.5% shape fixity and 93.5% shape recovery could be achieved when the specimen was deformed at 90°C, fixed at 45°C and recovered at 90°C in sample DMAPS20. This shape memory behaviour is generally called dual-SME since the shape is changed from one temporary shape to the permanent shape. It thus confirms that p(DMAPS-co-AA) with lower DMAPS-content show good dual-SME. Moreover, the dual-shape-memory effect could be repeated well because good shape fixity and shape recovery are both kept during the dual-shape-memory cycles (**Figure 8A**). Additionally, the sample DMAPS20 is also found to show excellent triple-SME,[69, 70] (**Figure 8B**). Figure 7B demonstrates that 33% elongation is obtained after 47% strain is deformed at 100°C due to the higher fixing temperature at 70°C. Whereas the strain fixity can reach 100% when 101% strain is deformed at 70°C and fixed at 20°C in the second fixing stage, which subsequently recovers from 101% to 32% upon a temperature increase from 20°C to 70°C, suggesting good shape recovery in the first recovery

stage. When the temperature is increased to 100°C, another 24.2% strain is recovered; suggesting weak strain recovery in the second recovery stage. Finally, only 7.8% residual strain confirms the good triple-shape-memory performance of p(DMAPS-co-AA). As compared with the POSS-polycaprolactone polyurethane, the residual strain of polyurethane was quantified to be between 13 and 43%. This high residual strain was ascribed to the plastic deformation originating from the second tensile deformation at a higher temperature.[71] Additionally, the sequential fixation and recovery of p(DMAPS-co-AA) is comparably good. When three temporary shapes are fixed at 85°C, 60°C, and 0°C, they can recovered sequentially at 60°C, 85°C, and 110°C, respectively (**Figure 8C**). When a deforming strain is fixed at a relatively low temperature, e.g., 0°C, the fixed strain can also recover gradually as the temperature increases from 70°C to 80°C, 95°C, 110°C, 120°C **(Figure 8D).** Furthermore, **Figure 8E** visually confirms the shape fixation and corresponding shape recovery of sample DMAPS20. These observations make this zwitterionic polymer a good candidate for many potential applications, such as sequential warnings, auto feed, controlled drug release and sequential collection of electronic waste.[23] Considering the good biocompatibility and other biological properties of zwitterionic polymers (**Figure SI7, SI8, SI9, SI10**), the development of p(DMAPS-co-AA) could also greatly promote the applications of SMPs in biomedical fields.

3.5 Moisture-sensitive SME

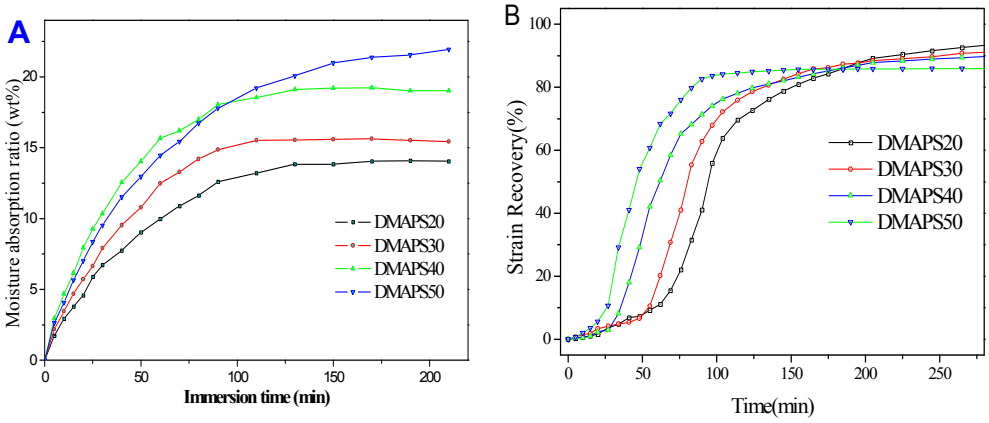

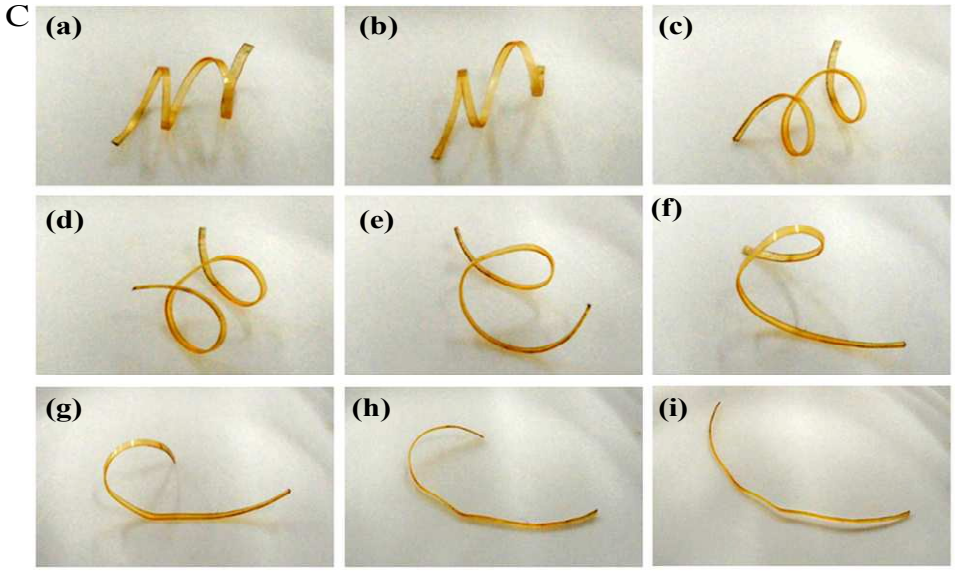

Figure 9. Moisture absorption curves (A) and moisture-sensitive strain recovery curves (B) of DMAPS-co-AA copolymer with different DMAPS contents under 80% RH and T=30°C;(C) moisture-sensitive shape recovery process of sample DMAPS50 under 80% RH and T=30°C ((a)0min; (b)10min; (c)20min; (d)30min; (e)40min; (f)50min; (g)60min; (h)70min; (i)80min)

Considering the biomedical applications, moisture-sensitive SME is more attractive since the shape recovery can be triggered by moisture or water stimulus, without heating the sample to a level unsuitable for biological conditions.[17, 59] Figure 9A demonstrates that the DMAPS-co-AA copolymers have good moisture absorption properties. All DMAPS-co-AA copolymers not only show very quick moisture absorption speed, but also high moisture absorption ratio. Within 100 minutes immersion time, most of the sample reaches its absorption balance and more than 13wt.% moisture absorption ratio can be obtained in the sample DMAPS20. Moreover, as the DMAPS content increases, the moisture absorption ratio increases significantly (see Figure 9A). These results provide the possibility to achieve good moisture-sensitive SME in the DMAPS-co-AA copolymers. This hypothesis was confirmed by the shape recovery curves of DMAPS-co-AA copolymers under the moisture condition of 80% RH and 30°C **(see Figure 9B).** When the DMAPS-content is lower than 60wt.%, all DMAPS-co-AA copolymers show good moisture-sensitive SME. Taking the sample DMAPS20 as an example, within 50 minutes, the temporary shape obtained by elongating

100% strain changed less than 8% strain. After immersing in moisture condition for 70 minutes, the strain recovered very quickly. Thereafter, the strain reached its balance slowly. Finally, the total shape recovery was higher than 90%. As the DMAPS content increases, the shape recovery shifts to lower immersion time, suggesting a quicker shape recovery in DMAPS-co-AA copolymers with higher DMAPS content. However, the sample with lower DMAPS-content tends to show higher shape recovery, e.g. 87% for DMAPS50, 89% for DMAPS40, 91% for DMAPS30, 93% for DMAPS20 (see Figure 9B). This observation is quite different from the pyridine containing polyurethane system exhibiting moisture-sensitive SME reported in previous literature.[17, 59] The possible reason is that samples with higher-DMAPS content have higher moisture absorption ratio as discussed in Figure 9A. Too much moisture or water molecules might destroy the ionic associations serving as physical netpoints, which is responsible for the shape recovery.[3] This is also the reason why the sample DMAPS60 shows a significantly lower shape recovery despite their high moisture absorption. Finally, the moisture-sensitive shape recovery process of sample DMAPS50 provides another intuitive proof to the moisture-sensitive SME of DMAPS-co-AA copolymers. A coiled-specimen was recovered to its original straight shape by immersing in moisture condition of 80% RH and 30°C (see Figure 9C). Though the inherent mechanism for moisture-sensitive SME would be investigated systematically in the following work, the moisture-sensitive shape memory functionality can greatly promote the application of DMAPS-co-AA copolymer in smart biomedical fields.

4. Conclusions

This paper reports the development of a novel zwitterionic copolymer having multi-SME and moisture-sensitive SME. Structure analysis confirms that the DMAPS-co-AA copolymer containing sulfobetaine groups are successfully copolymerized with DMAPS and AA. Morphology analysis further show that the DMAPS-co-AA copolymer forms a micro-phase separated structure. The strong hydrogen bonding among AA segments serve as reversible switches, while the strong electrostatic forces among DMAPS segments serve as physical netpoints. Thus, the DMAPS-co-AA copolymers not only show dual-SME, but also triple-SME. In addition to the thermal-induced SME, the DMAPS-co-AA copolymers also show moisture-sensitive SME. Considering the good biocompatibility and other biological

properties of zwitterionic polymers, we believe that p(DMAPS-co-AA) can greatly promote the application of SMPs in advanced biomedical fields, such as sequential warnings, auto feed, controlled drug release and sequential collection of electronic waste.

Acknowledgements

This work was financially supported by the National Natural Science Foundation of China (grant No. 21104045); the Special Research Foundation of Shenzhen Oversea High-level Talents for Innovation and Entrepreneurship (Grant No. KQCX20120807153115869), Nanshan District Key Lab for Biopolymers and Safety Evaluation (No.KC2014ZDZJ0001A), the Natural Science Foundation of Guangdong (grant No. S2013010013056, 2014A030313559), the Science and Technology Project of Shenzhen City (grant JCYJ20140828163633993), and the cultivate special funds of Guangdong province college students' scientific and technological innovation (special funds for climbing program).

References

1. G. J. Berg, M. K. McBride, C. Wang and C. N. Bowman, *Polymer*, 2014, **55**, 5849-5872.
2. W. M. Huang, B. Yang, Y. Zhao and Z. Ding, *J.Mater. Chem.*, 2010, **20**, 3367-3381.
3. J. Hu and S. Chen, *J.Mater. Chem.*, 2010, **20**, 3346-3355.
4. Y. J. Liu, H. B. Lv, X. Lan, J. S. Leng and S. Y. Du, *Compos. Sci. Technol.*, 2009, **69**, 2064-2068.
5. D. Ratna and J. Karger-Kocsis, *J. Mater. Sci.*, 2008, **43**, 254-269.
6. C. Liu, H. Qin and P. T. Mather, *J.Mater. Chem.*, 2007, **17**, 1543-1558.
7. L. Sun, W. M. Huang, C. C. Wang, Z. Ding, Y. Zhao, C. Tang and X. Y. Gao, *Liq. Cryst.*, 2014, **41**, 277-289.
8. A. Khaldi, J. A. Elliott and S. K. Smoukov, *J.Mater. Chem. C*, 2014, **2**, 8029-8034.
9. D. L. Safranski, K. E. Smith and K. Gall, *Polym. Rev.*, 2013, **53**, 76-91.
10. F. Wang, B. Zhu, L. Shu and X. Tao, *Smart Mater.Struct.*, 2014, **23**.
11. A. Y. N. Sofla, S. A. Meguid, K. T. Tan and W. K. Yeo, *Mater. Design*, 2010, **31**, 1284-1292.

12. Y. Liu, H. Du, L. Liu and J. Leng, *Smart Mater.Struct.*, 2014, **23**, 023001-023022.
13. M. Ecker and T. Pretsch, *RSC Adv.*, 2014, **4**, 46680-46688.
14. L. Sun, W. M. Huang, H. B. Lu, C. C. Wang and J. L. Zhang, *Assembly Autom.*, 2014, **34**, 78-93.
15. N. Fritzsche and T. Pretsch, *Macromolecules*, 2014, **47**, 5952-5959.
16. L. Sun and W. M. Huang, *Mater.Design*, 2010, **31**, 2684-2689.
17. S. Chen, J. Hu, C.W. M. Yuen and L. Chan, *Polymer*, 2009, **50**, 4424-4428.
18. W. M. Huang, B. Yang, L. An, C. Li and Y. S. Chan, *Appl. Phys. Lett.*, 2005, **86**.
19. Y. Zhu, J. Hu, H. Luo, R. J. Young, L. Deng, S. Zhang, Y. Fan and G. Ye, *Soft Matter*, 2012, **8**, 2509-2517.
20. W. Wang, H. Lu, Y. Liu and J. Leng, *J.Mater. Chem. A*, 2014, **2**, 5441-5449.
21. L. Sun and W. Huang, *Soft Matter*, 2013, **6**, 4403-4406.
22. K. Yu, T. Xie, J. Leng, Y. Ding and H. J. Qi, *Soft Matter*, 2012, **8**, 5687-5695.
23. T. Xie, *Nature*, 2010, **464**, 267-270.
24. T. Pretsch, *Smart Mater.Struct.*, 2010, **19**.
25. M. Bothe, K. Y. Mya, E. M. J. Lin, C. C. Yeo, X. Lu, C. He and T. Pretsch, *Soft Matter*, 2012, **8**, 965-972.
26. Y. Bai, X. Zhang, Q. Wang and T. Wang, *J.Mater. Chem. A*, 2014, **2**, 4771-4778.
27. L. Wang, X.F. Yang, H.M. Chen, G.Yang, T. Gong, W.B. Li and S.B Zhou, *Polym. Chem.-UK*, 2013, **4**, 4461-4468.
28. K. Suchao-in and S. Chirachanchai, *ACS Appl. Mater. Inter.*, 2013, **5**, 6850-6853.
29. J. Li, T. Liu, S. Xia, Y. Pan, Z. Zheng, X. Ding and Y. Peng, *J.Mater. Chem.*, 2011, **21**, 12213-12217.
30. I. Kolesov, O. Dolynchuk and H. J. Radusch, *Express Polym. Lett.*, 2015, **9**, 255-276.
31. C. Samuel, S. Barrau, J.M. Lefebvre, J.M. Raquez and P. Dubois, *Macromolecules*, 2014, **47**, 6791-6803.
32. Z. Wang, J. Zhao, M. Chen, M. Yang, L. Tang, Z.M. Dang, F. Chen, M. Huang and X. Dong, *ACS Appl. Mater. Inter.*, 2014, **6**, 20051-20059.
33. H. Meng, H. Mohamadian, M. Stubblefield, D. Jerro, S. Ibekwe, S.S. Pang and G. Li, *Smart Mater.Struct.*, 2013, **22**.

34. J. J. Li and T. Xie, *Macromolecules*, 2011, **44**, 175-180.
35. Y. Luo, Y. Guo, X. Gao, B.G. Li and T. Xie, *Adv. Mater.*, 2013, **25**, 743-748.
36. R. Dolog and R. A. Weiss, *Macromolecules*, 2013, **46**, 7845-7852.
37. F. Xuan and J. Liu, *Polym. Int.*, 2009, **58**, 1350-1361.
38. L. Mi and S. Jiang, *Angew.Chem.Int. Edit.*, 2014, **53**, 1746-1754.
39. A. B. Lowe and C. L. McCormick, *Chem. Rev.*, 2002, **102**, 4177-4189.
40. Y.-Y. Yuan, C.Q. Mao, X.J. Du, J.Z. Du, F. Wang and J. Wang, *Adv. Mater.*, 2012, **24**, 5476-5480.
41. W.H. Kuo, M.J. Wang, H.W. Chien, T.C. Wei, C. Lee and W.B. Tsai, *Biomacromolecules*, 2011, **12**, 4348-4356.
42. B. Cao, Q. Tang, L. Li, J. Humble, H. Wu, L. Liu and G. Cheng, *Adv. Healthc. Mater.*, 2013, **2**, 1096-1102.
43. R. Lalani and L. Liu, *Biomacromolecules*, 2012, **13**, 1853-1863.
44. A. Laschewsky, *Polymers-BASEL*, 2014, **6**, 1544-1601.
45. Y.H. Zhao, K.H. Wee and R. Bai, *ACS Appl. Mater. Inter.*, 2010, **2**, 203-211.
46. S. Zhai, Y. Ma, Y. Chen, D. Li, J. Cao, Y. Liu, M. Cai, X. Xie, Y. Chen and X. Luo, *Polym. Chem.-UK*, 2014, **5**, 1285-1297.
47. J.T. Sun, Z.Q. Yu, C.Y. Hong and C.Y. Pan, *Macromol. Rapid Comm.*, 2012, **33**, 811-818.
48. G. Li, G. Cheng, H. Xue, S. Chen, F. Zhang and S. Jiang, *Biomaterials*, 2008, **29**, 4592-4597.
49. Z. Zhang, S. Chen and S. Jiang, *Biomacromolecules*, 2006, **7**, 3311-3315.
50. D. Depan and R. D. K. Misra, *J. Biomed. Nanotechnol.*, 2015, **11**, 306-318.
51. L. Tauhardt, D. Pretzel, K. Kempe, M. Gottschaldt, D. Pohlers and U. S. Schubert, *Polym. Chem.-UK*, 2014, **5**, 5751-5764.
52. F. Cao, L. Tan, L. Xiang, S. Liu and Y. Wang, *J.Biomat. Sci.Polym. Edit.*, 2013, **24**, 2058-2070.
53. S. Chen, F. Mo, Y. Yang, F. J. Stadler, S. Chen, H. Yang and Z. Ge, *J.Mater. Chem. A*, 2015, **3**, 2924-2933.
54. C. Cummings, H. Murata, R. Koepsel and A. J. Russell, *Biomaterials*, 2013, **34**,

7437-7443.

55. N. Morimoto, K. Muramatsu, T. Wazawa, Y. Inoue and M. Suzuki, *Macromol. Rapid Comm.*, 2014, **35**, 103-108.
56. P. Yusan, I. Tuncel, V. Butun, A. L. Demirel and I. Erel-Goktepe, *Polym. Chem.-UK*, 2014, **5**, 3777-3787.
57. T. Ren, S. Yu, Z. Mao and C. Gao, *Biomaterials*, 2015, **56**, 58-67.
58. S. Chen, J. Hu and H. Zhuo, *J. Mater. Sci.*, 2011, **46**, 6581-6588.
59. S. Chen, J. Hu and S. Chen, *Polym. Int.*, 2012, **61**, 314-320.
60. S. J. Chen, J. L. Hu, Y. Q. Liu, H. M. Liem, Y. Zhu and Y. J. Liu, *J.Polym. Sci. Polym. Phys.*, 2007, **45**, 444-454.
61. C. Yang, K. Sun, J. Liu, H. Wang and Y. Cao, *Polym. Int.*, 2010, **59**, 1296-1302.
62. J. Dong, J. Ding, J. Weng and L. Dai, *Macromol. Rapid Comm.*, 2013, **34**, 659-664.
63. L. Xian Kai, C. Li, Z. Yi Ping and D. Zhi Zhi, *J. Mater. Sci.*, 2010, **45**, 2703-2707.
64. X. L. Zhu, Y. R. Gu, G. J. Chen, Z. P. Cheng and J. M. Lu, *J.Appl. Polym. Sci.*, 2004, **93**, 1539-1545.
65. G. Q. Liu, C. L. Guan, H. S. Xia, F. Q. Guo, X. B. Ding and Y. X. Peng, *Macromol. Rapid Comm.*, 2006, **27**, 1100-1104.
66. H. L. Frisch, *Polym.Eng.Sci.* 1980, **20**, 2-13.
67. S. Chen, F. Mo, Y. Yang, F. J. Stadler, S. Chen, H. Yang and Z. Ge, *J.Mater. Chem. A* 2015, **3**, 2924-2933.
68. Y. Zhu, J. Hu, K.F. Choi, Q. Meng, S. Chen and K.W. Yeung, *Polym. Advan.Technol.*, 2008, **19**, 328-333.
69. S. Chen, J. Hu, C.W. Yuen, L. Chan and H. Zhuo, *Polym. Advan.Technol.* 2010, **21**, 377.
70. S. Chen, H. Yuan, S. Chen, H. Yang, Z. Ge, H. Zhuo and J. Liu, *J.Mater. Chem. A*, 2014, **2**, 10169-10181.
71. M. Bothe, K. Y. Mya, E. M. J. Lin, C. C. Yeo, X. Lu, C. He and T. Pretsch, *Soft Matter*, **8**, 965-972.

Caption of Figures and Table

Table 1. Composition of synthesized DMAPS-co-AA copolymer

Figure 1. Polymerization reaction of DMAPS-co-AA copolymers

Figure 2. Molecular structure analysis of DMAPS-co-AA copolymer

Figure 3. Thermal properties of DMAPS-co-AA copolymers

Figure 4. Illustration for molecular structure of DMAPS-co-AA copolymer

Figure 5. DMA curves of DMAPS-co-AA copolymers

Figure 6. AFM images (A- 3D height, B-3D phase) of sample DMAPS20

Figure 7. Thermal-induced dual-SME of DMAPS-co-AA copolymers

Figure 8. Thermal-induced multi-SMEs of DMAPS-co-AA copolymer

Figure 9. Moisture absorption curves (A) and moisture-sensitive strain recovery curves (B) of DMAPS-co-AA copolymer with different DMAPS contents under 80% RH and T=30°C;(C) moisture-sensitive shape recovery process of sample DMAPS50 under 80% RH and T=30°C

Development of zwitterionic copolymers with multi-shape memory effects and moisture-sensitive shape memory effects

Shaojun Chen[1], Funian Mo[1], Shiguo Chen[1], Zaochuan Ge[1], *Florian J Stadler*[1*], Haitao Zhuo[2*],

[1]*Shenzhen Key Laboratory of Special Functional Materials, Nanshan District Key Lab for Biopolymers and Safety Evaluation, College of Materials Science and Engineering, Shenzhen University, Shenzhen, 518060, China.* [2]*College of Chemistry and Chemical Engineering, Shenzhen University, Shenzhen, 518060, China.*

*Corresponding author: College of Materials Science and Engineering，Shenzhen University, Shenzhen 518060, China. Tel and Fax: +86-755-26534562. E-mail: S.J.Chen, chensj@szu.edu.cn; H.T.Zhuo, haitaozhuo@163.com;

For Table of Contents use only

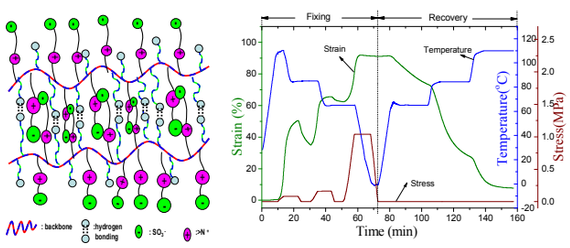

This paper develops a new kind of zwitterionic copolymer having multi-shape memory effect and moisture-sensitive shape memory effect from DMAPS and acrylic acid (AA). In addition to dual-SME, the copolymer also show triple-SME and quadruple-shape- memory effect.